Chapter 5

Optical Couplers

5.1 Introduction

Optoelectronics integrated circuits (OEICs) have progressed rapidly since the 1960s. For scaling down in integrated circuits, the waveguide structure in the OEIC requires a high refractive index contrast between waveguide layer and cladding layer. Among all the candidate platforms for waveguide structure applied in communication wavelengths, silicon-on-insulator (SOI) has been extensively investigated because of its good optical properties and compatibility with complementary metal-oxide-semiconductor (CMOS) fabrication processes. First, the absorption loss of SOI is relatively low in the infrared region and this is a critical property for optical communication and optical interconnect on chips. Secondly, the high refractive index contrast ($\Delta n \approx 2$) between the silicon core and silica cladding layers supports extreme light confinement and allows the waveguide core to be shrunk down to a submicron cross section. Besides, SOI is compatible with the microelectronics fabrication process, so low-cost monolithic integration of optical and electrical circuits is possible. All these properties ensure that SOI is a promising platform for OEIC [1]. These silicon circuits are also named photonic integrated circuits (PICs) due to the dense packing of optical functional devices and interconnects. Submicron

Silicon-Based Photonics
Erich Kasper and Jinzhong Yu

ISBN 978-981-4303-24-8 (Hardcover), 978-1-315-15651-4 (eBook)
www.jennystanford.com

waveguides can be utilized in many compact structures with outstanding performance [2, 3]. However, there are two challenges for its large-scale application in optical communication and computing systems:

- Single-mode waveguide is polarization sensitive. Fortunately, polarization independence can be obtained by deep-etched submicron rib waveguides [3].
- Optical coupling between an optical fiber and a nanophotonic waveguide causes a high insertion loss.

An essential question is how to couple light efficiently from the optical fiber to the PICs. As the SOI platform offers a high refractive index difference between core and cladding, the cross section of single-mode waveguides is a factor of $\sim 10^{-3}$ smaller than that of standard single-mode fibers and hence the large dimension mismatch induces large coupling losses. To bridge the gap between silicon PICs and the outside world, highly efficient coupling structures have to be developed, with the stringent conditions that they should be compact in size, broadband, and cost effective in fabrication.

The coupling loss between an optical fiber and a nanophotonic waveguide mainly consists of five parts: (i) lateral displacement loss, (ii) longitudinal transmission loss, (iii) axial tilting loss, (iv) modes mismatch loss, and (v) numerical-apertures mismatch loss. The preceding three loss mechanisms are caused by an alignment error, while the last two losses do not depend on the accuracy of alignment between the optical fiber and the nanophotonic waveguide. Typical optical fibers have mode sizes of the order of approximately 10 μm, contrasting greatly with the submicron size of Si-based submicron waveguides. The mismatch in both mode size and effective refractive index will result in radiation mode and back reflection from interfaces, which cause a high insertion loss for light coupling. Therefore, efficient optical coupling between an optical fiber and a nanophotonic waveguide is a key challenge for OEIC.

Several approaches for efficient light coupling have been proposed and experimentally demonstrated, the most popular approaches being tapered spot-size converters, prism couplers, and grating couplers. Table 5.1 lists different types of silicon-based optical couplers, including their coupling efficiency, bandwidths, and advantages and disadvantages.

Table 5.1 Comparison of different types of silicon couplers

	Coupling efficiency	Bandwidth	Advantage	Disadvantage
Tapered spot-size converters	Low	Very broad	Easy to fabricate	Large dimension, hard to integrate with a submicron waveguide, and of low coupling efficiency
Inverted tapered spot-size converters	Highest (90%)	Very broad	High alignment tolerance	Hard to fabricate and polarization sensitive
Inverted prism couplers	High (50%)	Broad	Easy to fabricate, flexible application, and reliable alignment	Hard to integrate, polarization sensitive, and extra epoxy adhesive
Graded index (GRIN) waveguide couplers	Very high (80%)	Broad	High fabrication tolerance	Hard to fabricate and integrate, low alignment tolerance, and high polarization sensitivity
Grating couplers	Very high	Broad	Easy to fabricate and integrate, high alignment tolerance, and no facet polishing	Polarization sensitive

A tapered spot-size converter has a very broad bandwidth but low coupling efficiency and a relatively large size, and it increases complexity for integration with a submicron waveguide. An inverted tapered spot-size converter offers the highest coupling efficiency—as much as 89%—but it is polarization sensitive and has stringent alignment tolerances and complex fabrication processes. A graded index (GRIN) waveguide coupler has high efficiency, of 78%, but it has stringent alignment tolerances and complex fabrication processes; it is also polarization sensitive. A grating coupler is relatively easy to fabricate and integrate. It has a high alignment tolerance and needs no facet polishing.

Inverted tapered spot-size converters [4] reported by IBM offered a very impressive coupling loss of only 0.5 dB per interface. Grating couplers [5] developed by Ghent University have solved the problem of the big mismatch between optical fiber and nanophotonic waveguide in dimension and realized vertical light coupling.

Light couplers are essential components of both optical interconnects and silicon photonics systems. In this chapter, working principles and properties of different silicon couplers are introduced and compared with each other.

5.2 Spot-Size Converter

Tapered structure waveguides, with dimension and symmetry differences, are widely used in spot-size converters for light coupling, which can significantly reduce the mismatch caused by the refractive index. The coupling efficiency of tapered spot-size converters depends on mode match between optical fiber and waveguide, surface refraction, and roughness. The mode mismatch can especially introduce a high insertion loss.

Tapered structure waveguides can convert the large mode spot-size of an optical fiber into a small mode spot-size so that the light can be coupled better into a nanophotonic waveguide, or vice versa. Typically, there are two kinds of spot-size converters: tapered and inverted. Not only the mode size but also the mode shape can be changed. This helps realize the perfect match between fiber optical mode and waveguide optical mode and improve light coupling efficiency accordingly. Tapered spot-size converters are intuitively the most obvious structures as their width changes gradually.

This allows a match between an optical fiber and a nanophotonic waveguide. Usually, tapered spot-size converters can be classified as lateral [6, 7], vertical [8–14], and combined (tapered both vertically and laterally) tapers [15, 16]. It has been demonstrated that inverted tapered [17–19] and slot-waveguide structures [20] are also spot-size converters.

5.2.1 Tapered Spot-Size Converters

On Optical Fiber Communication Conference 2003, Bookham's group first reported a vertical tapered spot-size converter for light coupling between optical fibers and SOI electronically variable optical attenuators; its coupling loss was only 0.5 dB per interface [6]. On the basis of Bookham's research, the Institute of Semiconductors, Chinese Academy of Sciences, made some improvements on its square rib structure and divided it into an upper rib and a middle rib, as shown in Fig. 5.1 [7].

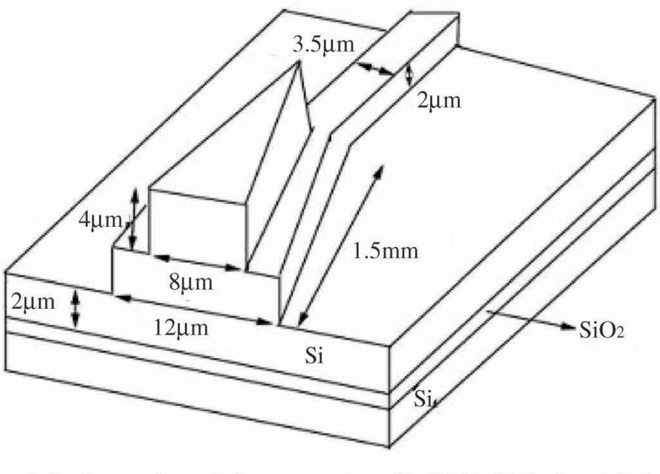

Figure 5.1 Tapered spot-size converter. © 2005 IEEE. Reprinted, with permission, from Ref. [7].

As a tapered spot-size converter, its end widths should be close to an optical fiber and a nano-optical waveguide, to avoid optical mode mismatch, which can cause a lot of insertion loss on taper connection between fibers and waveguides. When the light couples into the tapered spot-size converter, it first scatters across the three layers of the waveguide structure, which is as thick as 8 μm. Then it gradually focuses on the middle rib and the planar waveguide. Finally, it steadily propagates in the single-mode rib waveguide and the mode converting process ends in this tapered spot-size converter.

The insertion loss of the spot-size converters depends on their length and end width. The longer the spot-size converter, the lesser is the insertion loss and the slower is the optical mode converting process. The wide end of the converter will introduce a high additive loss by the light leakage. Simulation analyses have shown that the insertion loss, including the transmission loss in tapers, the coupling loss with the fiber, and the refraction loss at the interface, was 1.81 dB, in which coupling loss with the fiber was only 0.44 dB. Compared with direct light coupling from an optical fiber to a single-mode nano-optical waveguide, where the insertion loss is approximately 9 dB when alignment condition is the best, a tapered spot-size converter can reduce 7 dB of the insertion loss between an optical fiber and a nano-optical waveguide.

This kind of spot-size converter has shown very high coupling efficiency. However, there are still some problems, which limit its application. To avoid light leakage, the tapered spot-size converter is designed to be so long (1500 μm) that monolithic integration becomes unattractive. The upper rib is 4 μm high and easy to break during the fabrication and test processes. To reduce reflection loss of this spot-size converter, an antireflection coating is necessary for the light input and output port. Furthermore, polarization sensitivity limits its application, too.

Figure 5.2 shows a 3D adiabatically tapered structure [8], which can efficiently couple light from an optical fiber or free space to a chip. This structure of optical waveguides was fabricated directly on an SOI wafer. Fabrication processes included (i) writing a single grayscale mask by using a high-energy electron beam on a high-energy-beam-sensitive glass, (ii) ultraviolet grayscale lithography, and (iii) inductively coupled plasma etching. The input and output facet dimensions were 10 μm, approximately equal to the core diameter of a single-mode fiber. Its coupling efficiency increased with taper length for a given central waveguide as a result of the gradual mode conversion. The cross-sectional variation of the tapers was limited to vertical tapering because of the resolution constraints of the thick resist, so it did not achieve horizontal mode conversion. However, this did not limit its applicability. The tapering geometry was fixed to linear tapers to simplify fabrication, but the developed process could be easily extended to other geometries, such as sinusoidal or quadratic tapers. It should be pointed out that the coupling efficiency can be high by optimizing geometry if the taper is sufficiently long (>600 μm).

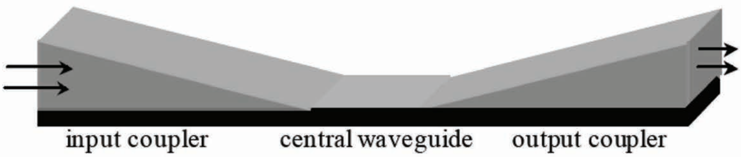

Figure 5.2 3D adiabatically tapered spot-size converter. Reprinted with permission from Ref. [8] © The Optical Society.

An ideal structure of the spot-size converter is the one that adiabatically tapers in both vertical and lateral directions; it can also be monolithically integrated with the OEIC. However, such structures cannot be achieved with standard lithography techniques. Confluent Photonics Inc. has fabricated such structures by gray tone lithography [15] and polishing [16], respectively. However, gray tone lithography introduces high losses due to misalignment and the polishing process could not be used in integrated fabrication of OEIC.

To fabricate vertically tapered structures, the dip-etch process [9], the dynamic etch mask technique [10], diffusion limited etch [11], and stepped etching [12] have been reported. All these methods have disadvantages of either low reproducibility or labor-intensive processing. Other techniques, like dry etching by a shadow mask [13], have been used in fabricating vertical tapers, but they do not allow processing on the wafer scale. Fabrication processes of the tapered spot-size converter of Fig. 5.2 are rather complex, but this converter is well suited for dense wafer-scale integration, so it can be further processed to realize other OEIC components. Its measured coupling efficiency of 45%–60% was lower than the theoretically expected value of 82%, mainly resulting from the scattering losses caused by surface roughness. As other tapered spot-size converters, antireflection coatings were used to prevent back reflection from the facets. This added complexity and cost. Furthermore, the minimization of the taper structure could cause serious surface roughness, resulting in higher back reflection and insertion loss.

5.2.2 Inverted Tapered Spot-Size Converters

According to single-mode condition, a strong light confinement effect can be achieved in a typical SOI single-mode waveguide where the mode profile is concentrated in the waveguide core and its effective refractive index approximately equals that of the silicon. However, the light confinement effect tends to be weak with the shrinking waveguide dimensions. When the waveguide is less than 150 nm wide, this confinement is very limited. An inverted tapered spot-size converter consists of a waveguide laterally tapered to a nanometer-sized tip at the facet in contact with the fiber. At the tip the mode field profile becomes delocalized from the waveguide core. And this delocalization of the mode field profile increases the mode overlap with the optical fiber mode. In addition, most of the mode field resides in the SiO_2 cladding region at the tip, causing the effective index to be close to that of the fiber, which results in negligible back reflections and high coupling efficiency.

A research group of Cornell University proposed and demonstrated an inverted tapered spot-size converter as shown in Fig. 5.3 [17]. It was a nano-optical waveguide laterally tapered to a nanometer-sized tip at the facet in contact with the fiber. The nanotaper and waveguides were fabricated on an SOI wafer with a SiO_2 layer as an optical buffer. SOI provides high-index difference and permits compatibility with integrated electronic circuits. The power overlap and the mode mismatch loss depend on the tip width for both transverse electric (TE)- and transverse magnetic (TM)-like modes. When the tip is 50 nm wide, the mode mismatch loss is only 0.4 dB. To convert the low-confined local mode at the nanotaper tip into the high-confined waveguide mode, a short tapered transition was employed by gradually varying both sidewalls in a symmetric parabolic transition toward the final waveguide width, where the parabola vertex is located at the nanotaper tip. Therefore, the taper length, which is necessary to convert the mode, also depends on the width of the nanotaper tip.

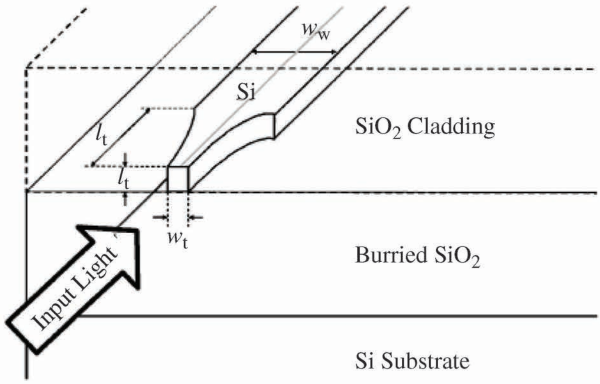

Figure 5.3 Inverted tapered spot-size converter by Cornell's group. Reprinted with permission from Ref. [17] © The Optical Society.

This kind of inverted tapered spot-size converter had a well-considered structure. However, its insertion loss was still higher than 3 dB. Furthermore, it was very sensitive to the polarization state. Simulation showed that the insertion losses for TM-like and TE-like modes at 1550 nm were 3.3 dB and 6 dB, respectively. The total measured insertion loss was 9.2 dB, including about 5 dB loss caused by the nano-optical waveguides, and this was quite close to the simulated result. The insertion loss originated from the mode mismatch loss between the optical fiber and tip facet modes and from mode conversion of the low-confined mode at the tip facet into the high-confined mode in the waveguide. Meanwhile, its misalignment tolerance was relatively large and the additional insertion loss for 1.2 μm misalignment in both horizontal and vertical directions was only 1 dB. This mainly resulted from the large field dimensions at the tip.

Several inverted tapered spot-size converters with good properties have been proposed and demonstrated. An inverted tapered spot-size converter as shown in Fig. 5.4 had only 1 dB measured mode conversion loss and 3.5 dB total insertion loss [18]. Though the insertion loss is relatively high, the converter has the potential to be used as a building block for OEIC if the random scattering loss caused by the sidewall in the silicon waveguide can be reduced. An inverted taper of similar structure with a very impressive coupling loss of only 0.5 dB was reported [19]. Among the reported SOI tapered or inverted tapered spot-size converters, different coupler solutions optimize either small footprint or high coupling efficiency or simple fabrication processes. However, the insertion efficiency is polarization sensitive.

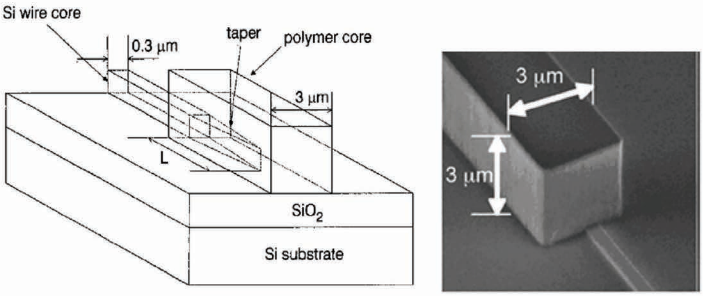

Figure 5.4 Schematic diagram of an inverted tapered spot-size converter. Republished with permission of Institution of Engineering and Technology (IET), from Ref. [18]. Copyright (2002); permission conveyed through Copyright Clearance Center, Inc.

5.2.3 Slot-Waveguide Spot-Size Converter

The slot-waveguide spot-size converter shown in Fig. 5.5 realizes a novel optical fiber-to-waveguide coupler concept [20]. It consists of an SOI substrate, slot waveguides, and cladding layers.

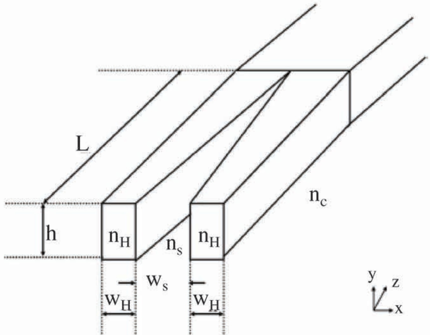

Figure 5.5 Schematic of the slot-waveguide spot-size converter. Reprinted with permission from Ref. [20] © The Optical Society.

The effective refractive index of this slot-waveguide structure is close to that of the standard single-mode fiber. The gap of the slot was tapered to be less than 150 nm at the facet in contact with the fiber where the mode field size increased because of the mode delocalization. The overlap of the mode fields of waveguide and fiber was enhanced, and optical low loss coupling from a fiber to the slot waveguide could be achieved accordingly.

To satisfy the continuity of the normal component of electric flux density, Maxwell's equations state that the corresponding electric field must undergo a large discontinuity with a much higher amplitude on the low-index side for a high-index-contrast interface. So discontinuity in the slot waveguide can be used to strongly enhance and confine light in a nanometer-wide region of a low-index material. The light fields overlap on the low-index side and localize to both slot waveguides finally. Therefore, high-efficiency light coupling is obtained.

The mode conversion loss of the slot-waveguide spot-size converter is relatively low. Simulated mode conversion loss with the air taper was less than 0.5 dB for a TE-like mode when the length of this converter was less than 90 nm. Furthermore, the mode conversion loss was negligible for the TM-like mode. The theoretical insertion loss was 1.8 dB, which mainly originates from mode mismatch at the facet.

The Institute of Microelectronics of Singapore presented a slot-waveguide spot-size converter for light coupling between a fiber and a submicron silicon nitride waveguide [21]. The coupling efficiency of the fabricated double-tip coupler was improved by as much as over 2 dB per coupling facet. This slot-waveguide spot-size converter has small dimensions but high coupling efficiency; its fabrication scheme is compatible with CMOS processes. However, the complexity of the fabrication processes, high requirements for the photoresist of electron beam lithography, and polarization sensitivity limit its widespread use.

5.3 Prism Coupler

5.3.1 Inverted Prism Coupler

Typically, a planar waveguide consists of three layers: cladding, guiding, and substrate. The imposition of the electromagnetic boundary condition leads to two physical conditions: total internal reflection in the guiding layer and a phase matching condition in each layer, which results in a set of discrete modes and their corresponding mode angles. With the prism coupler, guided waves with the appropriate mode angle can be introduced and high coupling efficiency can be achieved.

Figure 5.6 shows the schematic of inverted prism couplers [22]. The coupler incorporates the advantages of the vertically tapered spot-size converter and prism couplers and offers the flexibility for planar integration.

Polishing grayscale lithography or inductively coupled plasma (ICP) etching could be used to fabricate such kinds of structures on SOI substrates. The theoretical coupling efficiency is as high as 77%, and the measured coupling efficiency was 46% when it was coupled with a nanophotonic waveguide 0.25 m in diameter. The inverted prism had the advantages of flexible application, simple alignment process, high coupling efficiency, and broad 3 dB bandwidth (80 nm). However, an epoxy adhesive was needed for bonding with a nanophotonic waveguide. Besides, the inverted prism coupler was polarization sensitive and close to the waveguide, which easily disturbs the waveguide structures.

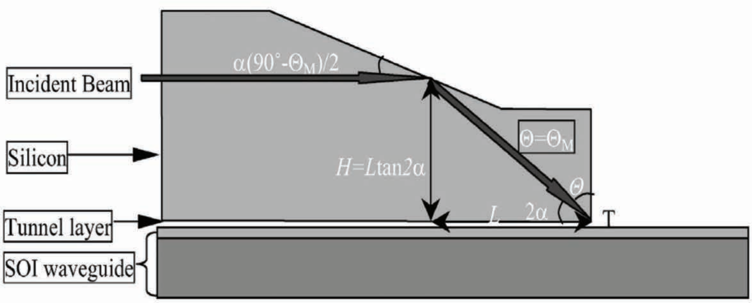

Figure 5.6 Schematic of an inverted prism coupler. Reprinted with permission from Ref. [22] © The Optical Society.

5.3.2 Graded Index Half-Prism Coupler

Figure 5.7 shows a GRIN half-prism coupler based on SOI. Its operation principal is similar to that of a conventional cylindrical

GRIN lens. Input light periodically converges in the SOI waveguide core and then diverges. The refractive index of an ideal planar GRIN waveguide lens decreases with a quadratic dependence on distance from the waveguide surface [23]. However, much simpler GRIN index profiles consisting of two or three uniform layers with a stepwise decreasing index profile perform almost as effectively as the ideal structure. Even the simplest case of a single uniform layer of a slightly lower index than the waveguide core could increase the optical power coupled into a small SOI waveguide from a fiber or a large input beam by several times.

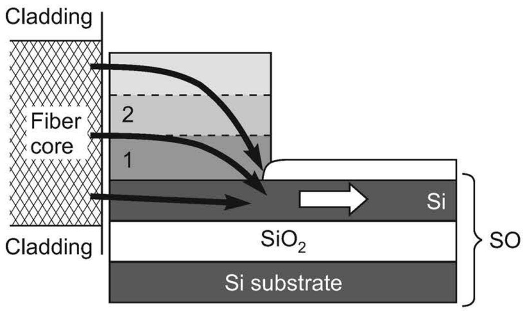

Figure 5.7 Schematic of the monolithic GRIN coupler structure.

Fabricating a GRIN coupler involved two key steps. The first was to deposit and pattern the a-Si GRIN layers on the SOI waveguide to form the coupler. The second was to create a lithographically defined input facet so that the correct coupler length was produced. Ridges were etched by reactive ion etching. The waveguide coupler sections were defined by etching a window in this SiO_2 layer over the waveguide adjacent to the eventual input facet position. The refractive index over the die area showed some spatial variation, ranging from 3.36 to 3.40. This index range is less than the index of Si, as required for effective GRIN lens focusing. The ICP etch process was developed to fabricate the input and output facets. To couple with a 0.5 μm silicon waveguide, the theoretical coupling efficiency was 71% and it could be increased to 78% by optimizing operation from a 4 μm thicker GRIN lens. The experimental and theoretical coupling efficiencies were in good qualitative agreement.

Besides the high light coupling efficiency, there are many other advantages of the GRIN coupler. The precision requirement for fabrication is only 1 μm, and a simple optical lithography process is qualified. Compared with the inversed tapered spot-size converter, the GRIN coupler does not need such an accurately thick cladding layer. The transmission loss in this coupler is negligible as its focal length is about 10 μm. However, the single layer GRIN coupler is sensitive to the mode shape of the input light and to the lateral misalignment of the fiber.

5.4 Grating Coupler

A grating coupler is a sort of novel solution to light coupling from an optical fiber to a nano-waveguide (and vice versa). Typically, there are both vertical [24–30] and horizontal [31–34] structures for light coupling. Grating couplers have a relatively high theoretical coupling efficiency. Nevertheless, the conventional grating couplers [32, 33] for OEIC have to overcome difficulties that stem from mode matching, the complexity of fabrication, the sensitivity to wavelengths, and the polarization state. Furthermore, the stringent light incident angle requirement needs special housings for packaged circuits or precise optical alignment for on-wafer measurements. However, the grating couplers have been investigated widely and improved significantly.

In the grating coupler with a horizontal coupling structure, the light from a fiber is directly coupled into a waveguide of a large cross section, then guided to a grating structure etched on this large wave-guide, and finally coupled into the small-dimension waveguide by diffraction. In the vertical coupling structure, a 2D spot-size converter is needed for the light coupling between a nanophotonic waveguide and a large cross-section waveguide in which the light is coupled from a fiber by the grating structure.

Grating couplers offer the following advantages:

- There is no need for additional wafer cleaning and facet polishing, which prevents not only complex post processes but also the potential threat to the circuits.
- Alignment tolerances are relatively high because the coupling area of the grating is similar to the cross section (10 μm diameter) of an optical fiber.

- They enable wafer-scale tests of PICs because of the flexibility of light coupling in/out from OEIC.
- Fabrication is compatible with CMOS processes.

The grating is formed in a wide waveguide section by linear grooves with periodic submicron spacing. The fabrication of the grooves utilizes techniques and processes applied in microelectronics manufacture, lithography, and etching for pattern formation.

5.4.1 Grating Coupler with a Vertical Coupling Structure

As mentioned above, the grating couplers with a vertical coupling structure should work with the spot-size converter. The light from a fiber is coupled into the waveguide of a large cross section by a grating structure, and then the spot-size converter can realize the mode match between the nanophotonic waveguide and the large cross-section waveguide. The fiber is aligned nearly perpendicular to the waveguide surface, and light coupling between an optical fiber and a nanophotonic waveguide is achieved.

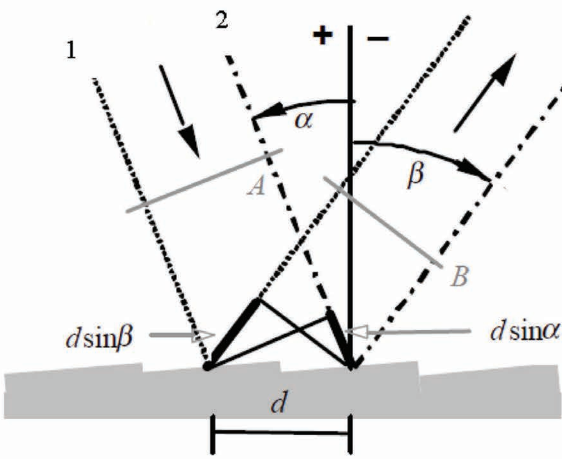

Figure 5.8 Illustration of a diffraction grating.

As shown in Fig. 5.8, parallel rays of monochromatic radiation from a single beam in the form of ray 1 and ray 2 are incident on a diffraction grating at angle α. These rays are then diffracted at angle

β. If the total path difference between ray 1 and ray 2 is equal to an integer multiple of the wavelength, constructive interference occurs. That is,

$$d(\sin\alpha + \sin\beta) = m\lambda, \tag{5.1}$$

where d is the grating period, the integer m is the diffraction order and $\lambda = \lambda_0/n_{\text{eff}}$, λ_0 is the vacuum wavelength, and n_{eff} is the effective refractive index of the dielectric. Equation 5.1 is the general grating equation.

When the incident illumination is perpendicular to the grating surface, that is, the incident angle $\alpha = 0$ and the diffracted angle $\beta = 90$, the grating formulation of Eq. 5.1 reduces to

$$d\, n_{\text{eff}} = m\lambda_0, \tag{5.2}$$

that is the diffraction grating equation for normal incidence. After incidence of light on a proper designed grating, the diffracted light is parallel to the grating surface direction and thereby can couple into the parallel nanophotonic waveguide. This is how the grating couplers of a vertical coupling structure work.

Equation 5.1 describes the relationship between the grating period, the effective refractive index of the dielectric, and the operating center wavelength. All these should be carefully considered for grating design. For convenience, only the first-order diffraction (m = 1), which contributes most to the light coupling, is considered.

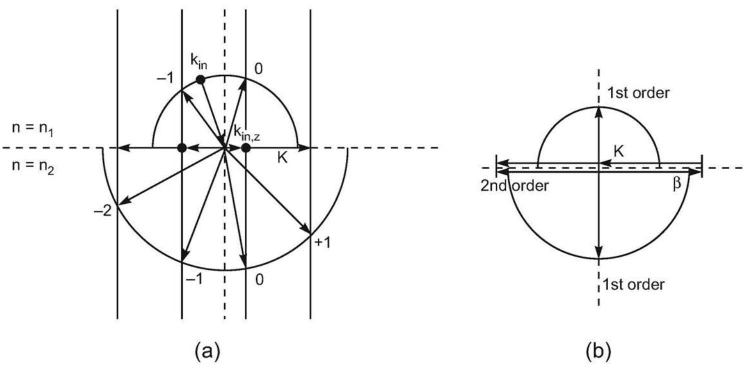

Figure 5.9 (a) A wave vector diagram for Bragg condition diffraction and (b) a wave vector diagram for second-order diffraction.

The Bragg condition is the most fundamental formula concerning periodic structures. As is shown in Fig. 5.9a, the Bragg condition describes the relation between the wave vectors of the incident and diffracted waves. If a grating consists of two materials with different refractive indexes and has the same period along the *z* axis, the Bragg equation is

$$k_z = k_{in,z} + mK, \tag{5.3}$$

where $k_{in,z}$ is the *z* component of $k_0 n_1$ in material 1, k_z is the *z* component of $k_0 n_2$ in material 2, and $K = \frac{2\pi}{d}$. This equation suits all kinds of grating structures, but for a waveguide grating coupler, a similar formula, in which the incident wave is replaced by the guided mode of the waveguide, can be used. It is:

$$k_{in,z} = \beta - mK, \tag{5.4}$$

where $\beta = \frac{2\pi}{\lambda_0} n_{eff}$. Equation 5.4 agrees with Eq. 5.2 for vertical incidence because then the in-plane component of the incoming wave $k_{in,z}$ is 0. But Eq. 5.4 also describes the coupling of light from an oblique alignment of the fiber with a finite component $k_{in,z}$. For a given grating period length *d*, the wavelength of the diffracted light can be changed by varying the inclination angle. The output of light from the waveguide to the fiber obeys the same laws. Figure 5.9b shows the wave vector diagram of a second-order grating for a waveguide grating coupler with a parallel guided wave. In this case, the first-order diffraction is vertically coupling both up and down out of the waveguide. Therefore, if light from the waveguide is diffracted by the grating structure etched on the waveguide, the diffraction wave up out of the waveguide can be coupled into an optical fiber.

The grating couplers usually consist of a grating structure of hundreds of micrometers. The coupling efficiency can be as high as 70% [31]. However, this is only the power that is coupled out of the waveguide, and not the coupling efficiency to fiber. When such a long grating structure is used, a curved focusing grating can be used to couple to a fiber. Though the output coupling efficiency is relatively high, the bandwidth of this kind of long grating coupler is narrow, which is caused by the small coupling strength.

The group from Ghent first reported an out-of-plane grating coupler for vertical coupling between 240-nm-thick GaAs–AlO_x waveguides and single-mode fibers [24]. In 2007, they proposed and demonstrated a grating coupler of only 10 μm length in SOI, as shown in Fig. 5.10 [25]. This SOI grating coupler had a Si core layer of 220 nm and a buried oxide layer of 1 μm. The etch depth was 70 nm, and the grating period was 630 nm. After grating diffraction, besides reflected and transmitted wave, there were upward- and downward-propagating waves. Since the coupling strength resulting from a deep etched groove is large enough, the light power was mostly contained in the upward- and downward-propagating waves. Thereby, the coupling efficiency mainly depends on the light power contained by the upward-propagating wave. The grating directionality is defined as the ratio between the optical power diffracted toward the fiber and the total diffracted optical power. High grating directionality is important to achieve a high coupling efficiency.

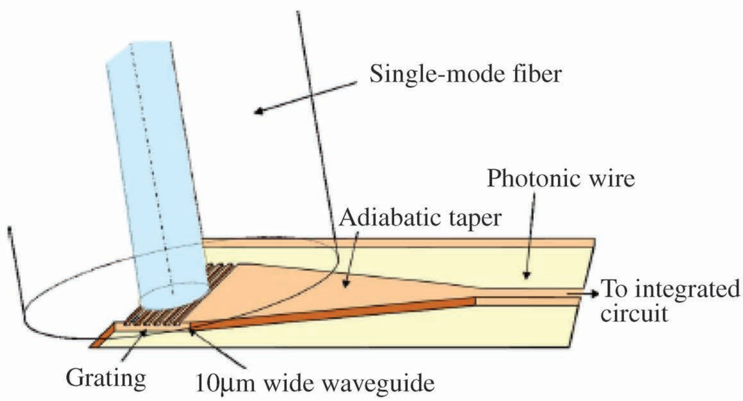

Figure 5.10 Schematic of Ghent's grating coupler. © 2005 IEEE. Reprinted, with permission, from Ref. [25].

The thickness of the buried oxide layer influences the efficiency of SOI grating couplers as the downward-propagating wave partially reflects at the oxide-substrate interface and interferes with the direct upward wave. When the thickness of the SiO_2 buried oxide layer changed from 900 nm to 1150 nm, the coupling efficiency rose from 22% to 64%. Compared with the long grating coupler, the coupler with a short grating structure was more compact and no focusing lens was needed. It was easy to fabricate with only one additive lithography process. Besides, it had a relatively wide bandwidth (1 dB bandwidth of 40 nm). It was compatible with CMOS manufacturing processes and easy to arrange with the single-mode fiber for on-wafer or on-chip tests.

To increase light coupling efficiency, it is necessary to enhance the grating directionality. One technical solution is to increase the light reflection at the interface in order to reduce the intensity of the downward-propagating wave. The research group of Ghent University proposed and demonstrated a high-efficiency grating coupler by using a bottom metal mirror as a reflector [26]. Benzocyclobutene (BCB), a low-index (n = 1.54 at λ = 1.55 μm) polymer, was chosen as the buffer layer. The optimum simulated BCB buffer thickness was 840 nm. Its thickness was optimized in order to get a constructive interference between the directly upward-radiated wave and the reflected wave at the bottom mirror. The SOI structure, covered with a metal mirror, was bonded onto a host substrate with another BCB layer, and finally, the Si substrate was removed. Compared with a conventional grating coupler, it was an upside-down structure and the grating directionality was almost 100% due to the perfect reflector of the bottom metal mirror. The measured light coupling efficiency to an optical fiber was 69%. The theoretical coupling efficiency was 90% after optimization of etched depth and grating period. However, the bottom metal mirror added more fabrication complexity, which was not compatible with CMOS fabrication processes.

The directionality of the grating diffraction can be improved by changing the structures of its grating as well as increasing the reflection from the substrate. The directionality of the upward diffraction is closely related to the thickness of the waveguide and the top silicon layer of SOI. A simulation had shown that a 370 nm thick waveguide and a 200 nm etch depth could realize enhanced directionality in SOI grating couplers.

Figure 5.11 shows a kind of grating coupler with a polysilicon layer reported by Ghent's group [27]. An additional polycrystalline silicon layer was deposited locally on the SOI substrate and the grating coupler was formed by etching the poly-Si layer as well as the top Si layer of the SOI substrate. The additive poly-Si layer modified the grating structure and enhanced the upward-propagating wave created by the grating. Therefore, it improved the grating directionality. The simulated coupling efficiency and 3 dB bandwidth of this structure were 78% and 85 nm, respectively. The measured coupling efficiency with a single-mode fiber was as high as 55% at 1550 nm [28]. It demonstrated that the coupler with a polysilicon layer enhances the grating directionality and thus raises the coupling efficiency. Furthermore, it is compatible with CMOS fabrication processes.

Conventional grating couplers are slightly inclined with respect to the vertical axis of the wafer surface. This prevents a large second-order back reflection into the SOI waveguide, which reduces the coupling efficiency. Both simulations and experiments have proven that the coupling efficiency of a tilted optical fiber can be 10% higher than that of vertical light coupling.

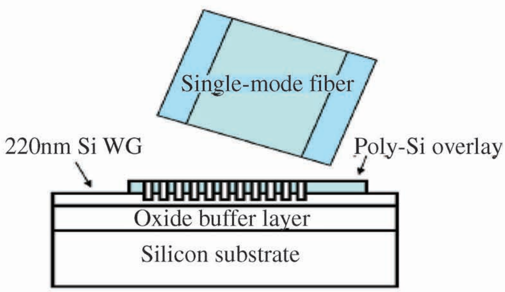

Figure 5.11 The grating coupler with a polysilicon layer. Reprinted with permission from Ref. [27] © The Optical Society.

OEIC chips are mounted in ceramic or plastic housings. Electrical contacts lead outside to contact pins, like in standard microelectronics packages. Optical contacts need fiber throughputs that are preferred for standard packaging in the horizontal or vertical direction. Vertical coupling with high directionality is a specific target mainly taking into account simple standard packaging.

A kind of vertical grating coupler with an extra slit was proposed and demonstrated [29]. Extra deep slits were fabricated by an additive lithography process after the ordinary grating structure was etched. The deep slits could suppress the second-order Bragg reflection from the grating. Theoretically, the couplers based on deep slits have a broad bandwidth and high coupling efficiency of 80% but the additive lithography process needed for the extra deep slit should be carefully designed and fabricated to achieve a high coupling efficiency. The short distance between the slit and the grating structure added complexity to fabrication processes.

A new kind of grating coupler made by relatively simple fabrication processes could obtain vertical light coupling [30]. Focused ion beam (FIB), which was used for a slanted grating structure, is a common tool for electronic device investigation and trimming. Use of gallium ions is standard in FIB. FIB is also useful for nanophotonics as it can be used to create complex 3D structures and accurate modification for nanostructures. However, it can introduce lattice damage and thereby high optical loss. Even the FIB with a low implantation dose causes an additive optical loss of 0.2–2 dB.

The vertical grating coupler garnered a lot of research interest due its high coupling efficiency, broad bandwidth, easy approach for integration, and compatibility with CMOS fabrication processes.

5.4.2 Horizontal Dual Grating–Assisted Coupler

Grating couplers can realize not only vertical light coupling but also horizontal light coupling between an optical fiber and a nanophotonic waveguide. An SOI dual grating–assisted directional coupler was reported by the group of Surrey [34]. The top layer was the SiON waveguide of a large dimension, which matched the optical fiber. The middle layer was the Si_3N_4 waveguide, which was used as a bridge between the SiON waveguide and the bottom SOI waveguide of a small dimension. This waveguide structure was fabricated one layer after another, and two grating structures were used for the light coupling between them. The refractive index of the SiON is 1.478, close to that of the optical fiber, resulting in less than a 0.05 dB insertion loss caused by a refractive index mismatch between the fiber and the waveguide. A fiber was butt-coupled to the thick SiON waveguide, and then the light was coupled into the Si_3N_4 waveguide using the first grating and subsequently coupled into the SOI waveguide via the second grating. The Si_3N_4 waveguide was important for highly efficient light coupling as it bridged the gap between SiON and the Si layer in terms of both refractive index and thickness. A thin SiON cladding layer was deposited on the Si_3N_4 and SOI waveguide to prevent leakage loss. Unibond 4-inch silicon wafers with a 3 μm buried SiO_2 layer and a 230 nm silicon top layer were used for the fabrication of this device. Plasma-enhanced chemical vapor deposition was used for the fabrication of SiON and Si_3N_4 layers. The silicon waveguide was fabricated by ICP etching, and the top three layers were structured by CHF_3 etching. A scanning electron micrograph of this device showed that the total height of SiON and Si_3N_4 layers suffered from overetching and therefore the maximum theoretical efficiency fell from 93% in the original design to 60% for the device as fabricated.

It is worth noting that for fabricating this horizontal dual grating–assisted directional coupler:

- The composition and thickness of the SiON should be carefully designed to match with the optical fiber and to reduce the insertion loss.
- The thickness of the intermediate Si_3N_4 should also be controlled carefully so that SiON and SOI waveguides match each other.
- The parameters of the grating structures, such as etch depth, length, and grating period, should be carefully designed to achieve a small device size and high coupling efficiency.

For fabrication, the growth of a multilayer structure and etching grating structure on the small-dimension waveguide are very difficult. Besides, the horizontal mode mismatch can cause an additive insertion loss.

The dual grating–assisted directional coupler is polarization insensitive when waveguide dimensions are properly designed and elastic stress is carefully controlled.

5.5 Conclusion

On a chip, the waveguide dimensions are small (submicron) whereas in the outer world, fiber waveguides dominate light transmission. The core of the fiber varies from about 10 μm diameter for a monomode fiber to 100 μm and more for a multimode fiber. The simplest butt coupling by horizontal alignment of fiber and nano-waveguide is very ineffective due to size and refractive index mismatch. Direct butt coupling is only used for qualitative experiments, and even then, it requires precise mechanical alignment of the fiber position. High-efficiency coupling needs special coupler structures. All the approaches for high-efficiency light coupling, including taped and inverted tapered spot-size converters, prism couplers and inverted prism couplers, and vertical and horizontal grating couplers, have been investigated widely, and from 2002 to 2008, the basic structures in SOI with good properties were demonstrated.

There are various kinds of silicon light couplers that have their own advantages, and they should be employed as building blocks integrated with other photonic devices according to their fabrication accuracy and complexity, coupling efficiency, and bandwidth. For the tapered spot-size converters, antireflection coatings are required to prevent back reflection from the facets. The taper should operate adiabatically; that is, the local first-order mode of the waveguide should propagate through the taper, while undergoing relatively little mode conversion to higher-order modes or radiation modes [35]. The inverted tapered spot-size converters have relatively small sizes, a high alignment tolerance, broad bandwidths, and high coupling efficiency. However, they are polarization sensitive, which hampers their application. For integration of waveguide devices and SOI active devices, inverted tapered spot-size converters of high coupling efficiency and relatively simple fabrication process are a good choice [36, 37]. A coupling efficiency of more than 90% can be achieved. The measured coupling efficiency of light coupling between an inverted tapered spot-size converter and a rib waveguide was raised to 0.7 dB by NTT [38].

Theoretical simulation shows very high coupling efficiency for grating couplers, but the structures of vertical grating couplers are complex. However, fabrication is possible using standard microelectronics process steps and planar surfaces without additional steps, such as facet polishing or bonding. The performance was improved to nearly perfect coupling within a decade. Manfred Berroth and coworkers at the University of Stuttgart give a good overview [39] about this development. They demonstrated a structure with a record measured efficiency of −0.62 dB at a wavelength of 1531 nm and a 1 dB bandwidth of 40 nm. The performance is enhanced through a backside metal mirror to enhance the directionality and an aperiodic grating that diffracts the field in a Gaussian-like form, improving overlap with the fiber mode.

Acknowledgments

We thank Hao Xu and Yu Zhu for the collection of basic information and figure drawings.

References

1. R. A. Soref and J. P. Lorenzo (1986). All silicon active and passive guided-wave components for λ = 1.3 μm and 1.6 μm, *IEEE J. Quantum Electron.*, **22**, 873–879.
2. Y. A. Vlasov and S. J. McNab (2004). Losses in single-mode silicon-on-insulator strip waveguide and bends, *Opt. Express*, **12**, 1622–1631.
3. L. Vivien, S. Laval, B. Dumont, S. Lardenois, A. Koster and E. Cassan (2002). Polarization-independent single-mode rib waveguides on silicon-on-insulator for telecommunication wavelengths, *Opt. Commun.*, **210**(1), 43–49.
4. S. J. McNab, N. Moll and Y. A. Vlasov (2003). Ultra-low loss photonic integrated circuit with membrane-type photonic crystal waveguides, *Opt. Express*, **11**, 2927–2939.
5. D. Taillaert, P. Bienstman and R. Baets (2004). Compact efficient broadband grating coupler for silicon-on-insulator waveguides, *Opt. Lett.*, **29**, 2749–2751.
6. I. Day, I. Evans, A. Knights, F. Hopper, et al. (2003). Tapered silicon waveguides for low insertion loss highly-efficient high-speed electronic variable optical attenuators, *Optical Fiber Communications Conference*, 249–251.
7. Y. Li, J. Yu and S. Chen (2005). Rearrangeable nonblocking SOI waveguide thermooptic 4×4 switch matrix with low insertion loss and fast response, *IEEE Photonics Technol. Lett.*, **17**, 1641–1643.
8. A. Sure, T. Dillon, J. Murakowski, C. Lin, D. Pustai and D. W. Prather (2003). Fabrication and characterization of three-dimensional silicon tapers. *Opt. Express*, **11**, 3555–3561.

9. T. Brenner, W. Hunziker, M. Smit, M. Bachmann, G. Guekos and H. Melchior (1992). Vertical InP/InGasAsP tapers for low-loss optical fiber-waveguide coupling, *Electron. Lett.*, **28**, 2040–2041.
10. M. Chien, U. Koren, T. L. Koch, B. I. Miller, M. G. Young, M. Chien and G. Raybon (1991). Short cavity distributed Bragg reflector laser with an integrated tapered output waveguide, *IEEE Photonics Technol. Lett.*, **3**, 418–420.
11. T. Brenner and H. Melchior (1993). Integrated optical modeshape adapters in InGaAsP/InP for efficient fiber-to-waveguide coupling, *IEEE Photonics Technol. Lett.*, **5**, 1053–1056.
12. G. Muller, G. Wender, L. Stoll, H. Westermeier and D. Seeberger (1993). Fabrication techniques for vertically tapered InP/InGasAsP spot-size transformers with very low loss, *Proc. Eur. Conf. Integrated Optics*, Neuchatel, Switzerland.
13. B. Jacobs, R. Zengerle, K. Faltin and W. Weiershausen (1995). Verticaly tapered spot size transformers by a simple masking technique, *Electron. Lett.*, **31**, 794–796.
14. L. Pavesi and D. J. Lockwood (2004). *Silicon Photonics* (Springer, Berlin).
15. www.confluentphotonics.com/technology/technical_papers.php#fabrication
16. J. J. Fijol, E. E. Fike, P. B. Keating, D. Gilbody, J. LeBlanc, S. A. Jacobson, W. J. Kessler and M. B. Frish (2003). Fabrication of silicon-on-insulator adiabatic tapers for low loss optical interconnection of photonic devices, *Proc. SPIE*, **4997**, Photonics Packaging and Integration III, https://doi.org/10.1117/12.479371.
17. V. R. Almeida, R. R. Panepucci and M. Lipson (2003). Nanotaper for compact mode conversion, *Opt. Lett.*, **28**, 1302–1304.
18. T. Shoji, T. Tsuchizawa, T. Watanabe, K. Yamada and H. Morita (2002). Low loss mode size converter from 0.3 μm square Si waveguides to singlemode fibres, *Electron. Lett.*, **38**, 1669–1700.
19. S. J. McNab, N. Moll and Y. A. Vlasov (2003). Ultra-low loss photonic integrated circuit with membrane-type photonic crystal waveguides, *Opt. Express*, **11**, 2927–2939.
20. Y. Liu and J. Yu (2007). Low-loss coupler between fiber and waveguide based on silicon-on-insulator slot waveguides, *Appl. Opt.*, **46**, 7858–7861.
21. S. H. Tao, J. Song, Q. Fang, M. Yu, G. Lo and D. Kwong (2008). Improving coupling efficiency of fiber-waveguide coupling with a double-tip coupler, *Opt. Express*, **16**, 20803–20808.

22. Z. Lu and D. W. Prather (2004). Total internal reflection–evanescent coupler for fiber-to-waveguide integration of planar optoelectronic devices, *Opt. Lett.*, **29**, 1784–1750.
23. S. Janz, B. Lamontagne, A. Delage, A. Bogdanov, D. X. Xu and K. P. Xu (2005). Single layer a-Si GRIN waveguide coupler with lithographically defined facets, *IEEE International Conference on Group IV Photonics*, 129–131.
24. D. Taillaert, W. Bogaerts, P. Bienstman, T. Krauss, P. Van. Daele, I. Moerman, S. Verstuyft, K. De Mesel and R. Baets (2002). An out-of-plane grating coupler for efficient butt-coupling between compact planar waveguides and single-mode fibers, *IEEE J. Quantum Electron.*, **38**, 949–995.
25. D. Taillaert, R. Baets, P. Dumon, W. Bogaerts, D. Van Thourhout, B. Luyssaert, V. Wiaux, S. Beckx and J. Wouters (2005). Silicon-on-insulator platform for integrated wavelength-selective components, *Proc. IEEE/LEOS Workshop Fibres and Optical Passive Components*, Italy, 115–120.
26. F. Laere, G. Roelkens, M. Ayre, J. Schrauwen, D. Taillaert and R. Baets (2007). Compact and highly efficient grating couplers between optical fiber and nanophotonic waveguide, *J. Lightwave Technol.*, **12**, 151–156.
27. G. Roelkens, D. Thourhout and R. Baets (2006). High efficiency Silicon-on-Insulator grating coupler based on a poly-silicon overlay, *Opt. Express*, **12**, 11622–11630.
28. G. Roelkens, D. Thourhout and R. Baets (2008). High efficiency diffraction grating coupler for interfacing a single mode optical fiber with a nanophotonic silicon-on-insulator waveguide circuit, *Appl. Phys. Lett.*, **92**, 131101–131103.
29. G. Roelkens, D. Thourhout and R. Baets (2007). High efficiency grating coupler between silicon-on-insulator waveguides and perfectly vertical optical fibers, *Opt. Lett.*, **32**, 1495–1497.
30. J. Schrauwen, F. Laere, D. Thourhout and R. Baets (2007). Focused-ion-beam fabrication of slanted grating couplers in silicon-on-insulator waveguide, *IEEE Photonics Technol. Lett.*, **19**, 816–818.
31. T. Ang, G. Reed, A. Vonsovici, A. Evans, P. Routly and M. Josey (2000). Effects of grating heights on highly efficient unibond SOI waveguide grating couplers, *IEEE Photonics Technol. Lett.*, **12**, 59–61.
32. J. K. Butler, N. H. Sun, G. A. Evans, L. Pang and P. Congdon (1998). Grating-assisted coupling of light between semiconductor and glass waveguides, *IEEE J. Lightwave Technol.*, **16**(6), 1038–1048.

33. R. Orobtchouk, N. Schnell, T. Benyattou, J. Gregoire, S. Lardenois, M. Heitzmann and J. M. Fedeli (2003). New ARROW optical coupler for optical interconnect, *IEEE International Conference on Interconnect Technology*, USA, 233–235.

34. G. Z. Masanovic, V. M. N. Passaro and G. T. Reed (2003). Dual grating-assisted directional coupling between fibres and thin semiconductor waveguides, *IEEE Photonics Technol. Lett.*, **15**, 1395–1397.

35. Y. Fu,, T. Ye, W. Tang and T. Chu (2014). Efficient adiabatic silicon-on-insulator waveguide taper, *Photon. Res.*, **2**, A41–A44.

36. K. K. Lee, D. R. Lim, D. Pan, C. Hoepfner, W. Oh, K. Wada, L. C. Kimerling, K. P. Yap and M. T. Doan (2005). Mode transformer for miniaturized optical circuits, *Opt. Lett.*, **30**, 498–500.

37. M. Galarza, D. Van Thourhout, R. Baets and M. Lopez-Amo (2008). Compact and highly-efficient polarization independent vertical resonant couplers for active-passive monolithic integration, *Opt. Express*, **16**, 8350–8358.

38. T. Tsuchizawa, K. Yamada, T. Watanabe, H. Fukuda, H. Nishi, H. Shinojima and S. Itabashi (2008). SSCs for rib-type silicon photonic wire waveguides, *Proc. IEEE Intern. Conf. Group IV Photonics*, Tokyo, 200–202.

39. W. Sfar Zaoui, A. Kunze, W. Vogel, M. Berroth, J. Butschke, F. Letzkus and J. Burghartz (2014). Bridging the gap between optical fibers and silicon photonic integrated circuits, *Opt. Express*, **22**, 1277–1286.